JOURNAL OF THERMOPHYSICS AND HEAT TRANSFER
Vol. 15, No. 3, July–September 2001

Effect of Film-Hole Shape on Turbine-Blade Film-Cooling Performance

Shuye Teng* and Je-Chin Han†
Texas A&M University, College Station, Texas 77843-3123
and
Philip E. Poinsatte‡
NASA John H. Glenn Research Center at Lewis Field, Cleveland, Ohio 44135-3191

Detailed coolant jet temperature profiles and film effectiveness distributions on the suction side of a gas turbine blade are measured using a thermocouple probe and a transient liquid crystal image method, respectively. The blade has only one row of film holes near the gill-hole portion on the suction side of the blade. The hole geometries studied include standard cylindrical holes and holes with diffuser-shaped exit portion (i.e., fan-shaped holes and laidback fan-shaped holes). Tests are performed on a five-blade linear cascade in a low-speed wind tunnel. The mainstream Reynolds number based on cascade exit velocity is 5.3×10^5. Upstream unsteady wakes are simulated using a spoke-wheel-type wake generator. The wake Strouhal number is kept at 0 or 0.1. Coolant blowing ratio is varied from 0.4 to 1.2. Results show that both expanded holes have significantly improved thermal protection over the surface downstream of the ejection location, particularly at high blowing ratios. In general, the unsteady wake tends to reduce film-cooling effectiveness.

Nomenclature

C_x = blade axial chord length (17 cm)
D = film-hole diameter
d = wake generator rod diameter
h = local heat-transfer coefficient
k = thermal conductivity of blade material (0.159 W/m · °C)
k_{air} = thermal conductivity of mainstream air
L = film-cooling hole length
M = coolant-to-mainstream mass flux ratio or blowing ratio, $\rho_c V_c/\rho_m V$
N = speed of rotating rods
Nu = local Nusselt number based on axial chord, hC_x/k_{air}
$\bar{N}u$ = spanwise-averaged Nusselt number
n = number of rods on wake generator
P = film-hole pitch
q'' = local forced convection heat flux with film injection
q_0'' = local forced convection heat flux for the no film-hole case
$\bar{q}''$ = spanwise-averaged forced convection heat flux with film injection
$\bar{q}_0''$ = spanwise-averaged forced convection heat flux for the no film-hole case
Re = Reynolds number based on exit velocity and axial chord, $V_2 C_x/\nu$
S = wake Strouhal number, $2\pi Ndn/(60V_1)$
SL = streamwise length on the suction surface (33.1 cm)
T_c = coolant temperature
T_f = film temperature
T_i = initial temperature of blade surface
T_m = mainstream temperature
T_w = liquid crystal color change from green to red
t = liquid crystal color change time
V = local mainstream velocity along the blade suction surface at the film-hole location
V_c = coolant hole exit velocity
V_1 = cascade inlet velocity
V_2 = cascade exit velocity
X = streamwise distance starting from film-hole centerline; streamwise distance measured from leading edge to film-hole centerline
Y = perpendicular distance from blade surface
Z = spanwise distance from centerline of film-cooling holes
α = thermal diffusivity of blade material (0.135×10^{-6} m²/s)
δ_2 = local momentum thickness
η = local film-cooling effectiveness
$\bar{\eta}$ = spanwise-averaged film-cooling effectiveness
θ = nondimensional coolant jet temperature $(T - T_m)/(T_c - T_m)$
ν = kinematic viscosity of cascade inlet mainstream air
ρ_c = coolant density
ρ_m = mainstream flow density
ϕ = overall cooling effectiveness given by $\phi = (T_m - T_w)/(T_m - T_c)$

Received 29 June 2000; revision received 22 January 2001; accepted for publication 23 January 2001.

*Research Assistant, Turbine Heat Transfer Laboratory, Department of Mechanical Engineering; currently Engineer, Heat Transfer Research, Inc., College Station, TX 77845.
†Marcus Easterling Chair Professor, Turbine Heat Transfer Laboratory, Department of Mechanical Engineering. Associate Fellow AIAA.
‡Research Engineer, Turbomachinery and Propulsion Systems Division.

Introduction

A CONTINUING trend toward higher gas turbine inlet temperatures that are sufficient to melt airfoils and endwalls and have resulted in higher heat loads on turbine components. Hence, sophisticated cooling techniques must be employed to cool the components to maintain the performance requirements. Some turbine blades are cooled by ejecting cooler air from within the blade through discrete holes to provide a protective film on the surface exposed to the hot gas path. Cooling jet injection may result in higher heat-transfer coefficients downstream of the injection location. However, the heat-transfer rates can still be substantially reduced as a result of a decreased film-to-wall temperature difference. Many studies have presented heat-transfer measurements on turbine blades with film cooling. Nirmalan and Hylton,[1] Abuaf et al.,[2] Ames,[3,4] and Drost and Bölcs[5] studied film-cooling heat transfer on film-cooled turbine vanes. Camci and Arts[6] and Takeishi et al.[7] studied film-cooling heat transfer on film-cooled turbine blades. Ito et al.[8] and Haas et al.[9] studied the effect of coolant density on film-cooling effectiveness on turbine blades.

The effect of unsteady wakes produced by upstream vane trailing edges has a strong effect on rotor blade surface heat-transfer coefficient distributions. Several studies have focused on the effect of

unsteady wakes on the downstream blade heat-transfer coefficient distributions without film cooling. They all reported that unsteady wakes enhanced turbine-blade heat transfer and caused earlier and longer laminar-turbulent boundary-layer transition on the suction surface. Few studies have focused on the effect of unsteady wakes on film-cooled turbine blades. Abhari and Epstein[10] conducted heat-transfer experiments on a film-cooled transonic turbine stage in a short-duration turbine facility. They measured steady and time-resolved, chordwise heat-flux distributions at three spanwise locations. They concluded that film cooling reduces the time-averaged heat transfer by about 60% on the suction surface compared to the uncooled rotor blade. However, the effect is relatively low on the pressure surface. Ou et al.[11] and Mehendale et al.[12] simulated unsteady wake conditions over a linear turbine-blade cascade with film cooling. They studied the effects of unsteady wake on a model turbine blade with multiple-row film cooling using air and CO_2 as coolants. They measured heat-transfer coefficients and film-cooling effectiveness at discrete locations using thin foil heating and multiple thermocouples. They concluded that heat-transfer coefficients increase and film-cooling effectiveness values decrease with an increase in unsteady wake strength. Du et al.[13,14] used a transient liquid crystal technique to measure the detailed heat-transfer coefficient and film effectiveness distributions over a film-cooled turbine blade under the effect of upstream unsteady wakes. They concluded that unsteady wake slightly enhances Nusselt numbers but significantly reduces film-cooling effectiveness on a film-cooled blade surface as compared to a film-cooled blade without unsteady wake. Teng et al.[15] studied unsteady wake effect on film temperature and effectiveness distributions for a gas turbine blade with one row of cylindrical film holes near the suction side gill-hole region. They concluded that unsteady wake reduces film-cooling effectiveness. They also found out that film injection enhances the local heat-transfer coefficient while the unsteady wake promotes earlier boundary-layer transition.

To improve the cooling effectiveness and thus increase the lifetime of gas turbine blades, an attempt has recently been made to contour the film-hole geometry. Film-cooling holes with a diffuser-shaped expansion at the exit portion of the holes are believed to improve the film-cooling performance on a gas turbine blade. The increased cross-sectional area at the hole exit compared to a standard cylindrical hole leads to reduction of the coolant velocity for a given blowing ratio. The momentum flux of the jet exiting the hole and the penetration of the jet into the mainstream will be reduced accordingly, which results in an increased cooling efficiency. Furthermore, lateral expansion of the hole provides an improved lateral spreading of the jet, which leads to a better coverage of the airfoil in the lateral direction and a higher laterally averaged film-cooling efficiency. A few previous studies have shown that expanding the exit of the cooling hole improves film-cooling performance in comparison to a cylindrical hole. Goldstein et al.[16] reported that overall improvements in adiabatic effectiveness are found for the flat-plate film cooling with laterally expanded holes. Makki and Jekubowski[17] reported that the same improvements are found for forward-expanded holes. Haller and Camus[18] performed aerodynamic loss measurements on a two-dimensional transonic cascade. Holes with a spanwise flare angle of 25 deg are found to offer significant improvements in film-cooling effectiveness without any additional loss penalty. Schmidt et al.[19] and Sen et al.[20] compared a cylindrical hole to a forward-expanded hole, both of them having compound angle injection for the flat-plate film cooling. Although the spatially averaged effectiveness for the cylindrical and forward-expanded holes is the same, a larger lateral spreading of the forward-expanded jet is found. Gritsch et al.[21,22] performed detailed measurements of the flat-plate film-cooling effectiveness and heat-transfer coefficients downstream of single holes for holes with expanded exits. They reported that, compared to the cylindrical holes, the two types of expanded holes in their study show significantly improved thermal protection of the surface downstream of the ejection location, particularly at the high blowing ratios. Bell et al.[23] show that the amount of expansion is critical to this improvement.

All of the preceding studies show that film-cooling holes with a diffuser-shaped expansion at the exit portion of the hole have improved film-cooling performance in comparison to cylindrical holes. It is of great interest to understand the effect of the hole shape on blade film-cooling performance under turbomachinery flow conditions, that is, consideration of the effect of surface curvature and pressure gradient that exists on a real turbine blade. However, most of the just-mentioned shape hole film-cooling studies are for flat-plate geometry. There are very few studies present in open literature examining the effects of hole shape on turbine-blade film-cooling performance under steady and unsteady wake conditions. This study focuses on only one row of film holes near the suction-side gill-hole portion in order to investigate the hole shape effect on the curved blade surface under strong flow acceleration conditions. Film-cooling holes with and without exit expansions are studied and compared under steady and unsteady wake conditions. In the present study a transient liquid crystal method is used to measure the detailed heat-transfer coefficient and film effectiveness distributions, and a thermocouple probe is used to measure coolant jet temperature profiles just above the gas turbine blade. The high resolution of the liquid crystal technique, combined with the coolant jet temperature profile measurement, provides a clear picture of how the heat-transfer coefficient and film effectiveness distributions vary along the blade surface with different film hole shapes. The results also provide a good database for film-cooling computational model development. The corresponding results of the detailed heat-transfer coefficient distributions are presented in an accompanying paper.[24]

Experimental Apparatus

Figure 1a shows the schematic of the test section and camera locations. The test apparatus consists of a low-speed wind tunnel with an inlet nozzle, a linear turbine-blade cascade with the test blade in the center, and a suction-type blower. The wind tunnel is designed to accommodate the 107.49-deg turn of the blade cascade. The cascade inlet mean velocity is about 20 m/s. The mean velocity increases 2.5 times from the inlet of the cascade to the exit. The test apparatus is

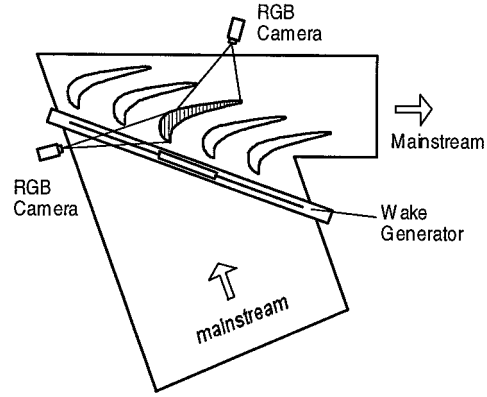

Fig. 1a Five-blade cascade with center blade coated with liquid crystal and viewed by two cameras.

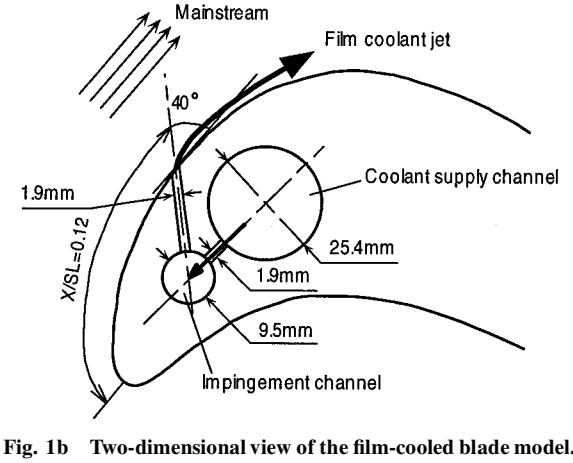

Fig. 1b Two-dimensional view of the film-cooled blade model.

described in detail by Ou et al.[11] A spoked-wheel-type wake generator, similar to the one used by Ou et al.,[11] simulated the upstream unsteady wake. The wake generator has 32 rods, each 0.63 cm in diameter, to simulate the trailing edge of an upstream vane. The wake Strouhal number is adjusted by controlling the rod rotation speed N. The error caused by using nonparallel rotating rods with a linear blade cascade is small and is discussed by Ou et al.[11] The blade configuration, scaled up five times, produces a velocity distribution typical of an advanced high-pressure turbine-blade row. The cascade has five blades, each with an axial chord length of 17 cm and a radial span of 25.2 cm. The blade spacing is 17.01 cm at the cascade inlet, and the throat-to-blade span ratio is 0.2. Du et al.[13] presented the local-to-exit velocity ratio distribution around the blade as well as the instantaneous velocity, ensemble-averaged velocity, and ensemble-averaged turbulence profiles at the cascade inlet under the effect of upstream unsteady wakes. The velocity on the suction side accelerates to about $X/SL = 0.5$ ($V/V_2 = 110\%$) and then decelerates slightly at the cascade exit. In the present study, a row of film holes is located near the suction-side gill-hole region $X/SL = 0.12$, where V/V_2 is estimated to be about 68%, the momentum thickness δ_2 is about 9×10^{-4} m, and the momentum thickness Reynolds number is estimated to be about 200 for steady flow. The unsteady wakes are actually velocity deficiencies caused by the blockage of mainstream flow by the rotating rods. The ensemble-averaged turbulence intensity profiles at the cascade inlet show that intensity could be as high as 20% inside the wake, but the time-mean-averaged turbulence intensity is about 10.4%. For cases without unsteady wake effect, that is, without the rotating rods in the mainstream flow, the time-mean-averaged turbulence is about 0.7%.

The present film-cooled turbine-blade model is the same as the one used by Teng et al.[15] Figure 1b presents a two-dimensional view of the film-cooled turbine-blade model. The blade material is Renshape. Its thermal conductivity is 0.159 w/m · k, and thermal diffusivity is 1.35×10^{-7} m^2/s. There is one cavity used to supply coolant to the row of film holes on the suction side. The film holes, 1.905 mm in diameter and 10.16 mm apart from one another ($P/D = 5.3$), have a radial angle of 90 deg and a tangential angle of 40 deg. The film-hole length is 15 mm ($L/D = 7.9$). The flow rate is controlled by a flow meter. The heated coolant flow is passed through a solenoid-controlled three-way diverter valve before the flow enters the coolant cavity inside the blade. The solenoid-controlled valve is connected to a switch that triggers the heated coolant flow into the cavity at the instant the transient test is initiated.

The film temperature distributions are measured by a traversing fine gauge thermocouple probe at $X/D = 5$ and 10 from the centerline of the film-cooling holes. The thermocouple bead size is about 0.01 cm and the probe size is about 0.0254 cm. The response time of this fine gauge thermocouple is 0.08 sec. The measuring plane is perpendicular to the oncoming mainstream. When measuring the film temperature field, the blade model is not heated, and only the coolant is heated and ejected. The mainstream temperature is 21.1°C. The coolant has been heated to about 43.3°C to reduce measurement uncertainty.

The liquid crystal coated surface area is 7.2 cm wide, and the data acquisition area is 2.5 cm wide along the midspan region of the test blade. In film-cooling measurements the test blade surface is heated uniformly using a heater box.[15] The heater box has the blade shape and is slightly larger than the test blade. The insides of the heater box are instrumented with thin foil heaters and controlled by using several variacs to provide a near uniform surface temperature. The heater box is lowered to completely cover the test blade during heating. The heater box is raised completely to expose the test blade to the mainstream during the transient test. The blade surface temperature is monitored using embedded thermocouples during heating. The uniformity of surface temperature with heating is within ±1.2°C. An interpolation scheme is used to further reduce the temperature variation in the initial surface temperature to within ±0.2°C. In the present study the blade surface is heated to a temperature above the liquid crystal blue color (37.2°C). The mainstream air is turned on by starting the suction-type blower. When the blower reaches the stable test flow conditions, the heater box is raised to expose the hot blade to the room temperature mainstream air within 0.1 s. When the heater box completely clears the blade height, the liquid crystal data acquisition system is automatically triggered. The liquid crystal color change time is measured using a high-precision image-processing system. The transient tests last about 60–90 s in average. The system consists of two cameras individually connected to a color frame grabber board in the personal computer and a monitor. Software is used to measure the time of color change of liquid crystals. During one test, only one camera is operational. Hence, we require two different runs with two different camera locations to measure one set of data on the suction side for a particular condition. Details on the image-processing system are presented by Teng et al.[15] The image-processing system consists of an RGB camera, monitor, and a personal computer with color frame grabber board.

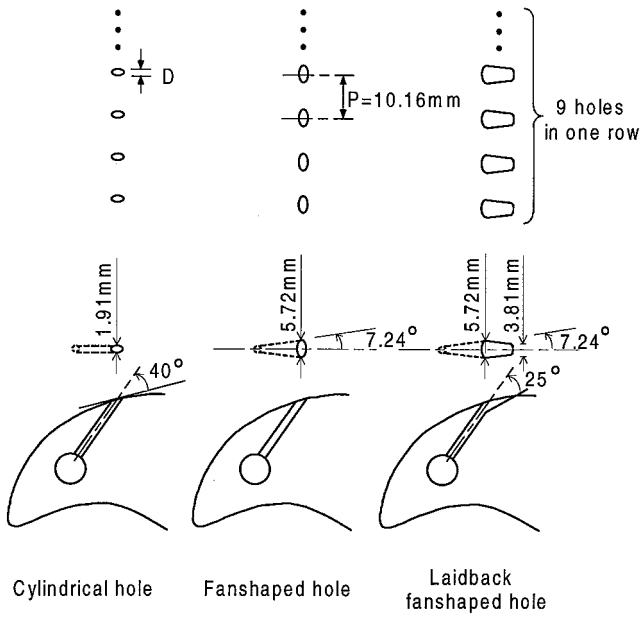

Fig. 2 Film-cooling hole geometries.

Figure 2 presents the three types of hole geometries studied: cylindrical hole, fan-shaped hole, and laidback fan-shaped hole. The same hole geometries as used by Teng et al.[24] are again used here. The hole geometries are similar to those used by Gritsch et al.[21] They have shown that, in flat-plate geometry, an expanded hole shows significantly improved thermal protection of the surface downstream of one hole ejection location as compared to one cylindrical hole. In the present study a row of nine holes of each shape located near the blade suction-side gill-hole region ($X/SL = 0.12$) are employed. The diameter of the cylindrical hole D and diameter of the cylindrical inlet section of the expanded hole is 1.91 mm. For all geometries the inclination angle is 40 deg, the pitch-to-diameter ratio is $P/D = 5.3$, and the length-to-diameter ratio L/D is 7.9. The lateral expansion angle of both expanded holes is 7.24 deg. The exit forward expansion angle of the laidback fan-shaped hole is 25 deg. For the fan-shaped and laidback fan-shaped hole the calculation of the blowing ratio is based on the inlet cross-sectional area of these holes, that is, the same as the cylindrical hole. In this study this means that the same blowing ratio provides the same amount of coolant ejected under the same mainstream condition. Thus, the blowing ratio of the shaped holes can be directly compared to those of the cylindrical hole, which makes it more convenient to evaluate the effect of the hole exit shape.

Data Analysis

A thermocouple probe is used to measure the detailed temperature profiles on the blade suction side. The local time-averaged temperature T profiles are presented as a nondimensional temperature θ defined similar to film effectiveness,

$$\theta = (T - T_m)/(T_c - T_m) \tag{1}$$

One-thousandtwo-hundreddata points are measured at each measurement plane at different X/D locations. At each data point 36,864 samples are acquired and averaged to get the time-averaged temperature.

A transient liquid crystal technique is used to measure the detailed heat-transfer coefficients and film-cooling effectiveness on the blade suction surface. The technique is similar to the one described by Teng et al.[15] A one-dimensional transient conduction into a semi-infinite solid with convective boundary condition is assumed. The solution for surface temperature is obtained as

$$(T_w - T_i)/(T_m - T_i) = \left[1 - \exp(h^2\alpha t/k^2)\,\mathrm{erfc}\left(h\sqrt{\alpha t}/k\right)\right] \quad (2)$$

where T_w is the wall temperature when liquid crystals change to red from green (32.7°C) at time t. The heat-transfer coefficient is obtained from Eq. (2). For film-cooling tests the mainstream temperature T_m in Eq. 2 is replaced by the local film temperature T_f, which is a mixture of the coolant T_c and mainstream temperatures. The film temperature is defined in terms of η, which is the film-cooling effectiveness.

$$\eta = (T_f - T_m)/(T_c - T_m), \qquad \text{or} \qquad T_f = \eta T_c + (1-\eta)T_m \quad (3)$$

For the film-cooling test we obtain an equation similar to Eq. (2):

$$\frac{T_w - T_i}{T_f - T_i} = \frac{T_w - T_i}{\eta T_c + (1-\eta)T_m - T_i} = \left[1 - \exp\left(\frac{h^2\alpha t}{k^2}\right)\mathrm{erfc}\left(\frac{h\sqrt{\alpha t}}{k}\right)\right] \quad (4)$$

Two similar transient tests are run to obtain the heat-transfer coefficient h and film-cooling effectiveness η. Each transient test lasts about 60–90 s in average. In the first test the blade surface is heated, and the coolant and the mainstream temperatures are nearly the same. In this case there is only one unknown h in Eq. (2). For the second test the coolant is heated to a temperature close to blade initial temperature. The calculated local heat-transfer coefficient from the first test is substituted in Eq. (4) to obtain the local film-cooling effectiveness. The methodology is described in detail by Teng et al.[15] The preceding equations are solved at each point on the blade surface (16,600 points) to obtain the detailed heat-transfer coefficient and film-cooling effectiveness distributions.

Because the objective of film injection is to reduce the heat transfer (heat load) to a gas turbine component, heat loads with film injection and for no film holes case should be compared. The local-heat-flux ratio (heat load ratio) is given by

$$q''/q_0'' = (h/h_0)[(T_f - T_w)/(T_m - T_w)] \quad (5)$$

where a heat-flux ratio of less than unity indicates that film injection reduces the surface heat load over the no film holes case.

Because it is very difficult to determine the local film temperature for a real gas turbine blade, Eq. (3) can be used to substitute for the film temperature. Equation (5) can then be rewritten as

$$q''/q_0'' = (h/h_0)[1 - \eta(x,z)/\phi] \quad (6)$$

For gas turbine blades the value of ϕ usually ranges from 0.5 to 0.7.

Spanwise-averaged heat-flux ratio is then obtained from

$$\frac{\bar{q}''}{\bar{q}_0''} = \frac{1}{n}\sum_{i=1}^{n}\frac{h(x,z_i)}{h_0(x,z_i)}\left[1 - \frac{\eta(x,z_i)}{\phi}\right] \quad (7)$$

where n is the number of data points in the row at the same streamwise location x, and z is the spanwise dimension. A typical value of 0.6 is chosen for ϕ. This analysis is the same as that by Mehandale and Han.[25]

The uncertainty in the coolant jet temperature field measurement using a thermocouple is estimated to be 1%. The average uncertainty in heat-transfer coefficient measurement is estimated to be ±6.5%. The individual uncertainties in the measurement of the time of color change ($\Delta t = \pm 5\%$), the mainstream temperature ($\Delta T_m = \pm 1.3\%$), the initial temperature ($\Delta T_i = \pm 0.6\%$), the color change temperature ($\Delta T_w = \pm 3\%$), and the wall material properties ($\Delta\alpha/k^2 = \pm 2\%$) are included in the calculation of the overall uncertainty in the measurement. The uncertainty in the film-cooling effectiveness measurement including the additional uncertainties in the heat-transfer coefficient measurement is estimated to be about ±9.2%. The uncertainty in the immediate vicinity of the hole (less than 1 diam around the hole) could be higher as a result of the two-dimensional conduction effect.

Results and Discussion

Experiments are performed at a cascade exit Reynolds number of 5.3×10^5. The corresponding flow velocity at the cascade exit is 50 m/s. Heated air as coolant is tested at blowing ratios of 0.4, 0.6, 0.8, and 1.2 for no-rod no-wake cases ($S = 0$, $\bar{T}u = 0.7\%$) and cases with wake ($S = 0.1$, $\bar{T}u = 10.4\%$). Because the film effectiveness distributions with the cylindrical hole have already been presented in Teng et al.,[15] here we focus on the film effectiveness distributions with the shaped holes.

Detailed Heat-Transfer Coefficient Measurements

Detailed heat-transfer coefficient distributions are presented in an accompanying paper.[24] Because of page limitation, the important conclusions are summarized as follows.

For steady flow, when compared with cylindrical holes, both fan-shaped and laidback fan-shaped holes have much lower Nusselt numbers right after the film injection location. However, they cause higher heat-transfer coefficients in the latter part of the blade surface as a result of earlier boundary-layer transition. For unsteady flow, when compared with cylindrical holes, both fan-shapedand laidback fan-shaped holes also have much lower Nusselt numbers right after the film injection location. They have almost the same boundary-layer transition location as the cylindrical hole case, but their Nusselt numbers are higher after transition into the turbulent region.

Detailed Film Effectiveness Measurements

Figures 3 and 4 present the detailed film effectiveness distributions at different blowing ratios for fan-shaped and laidback

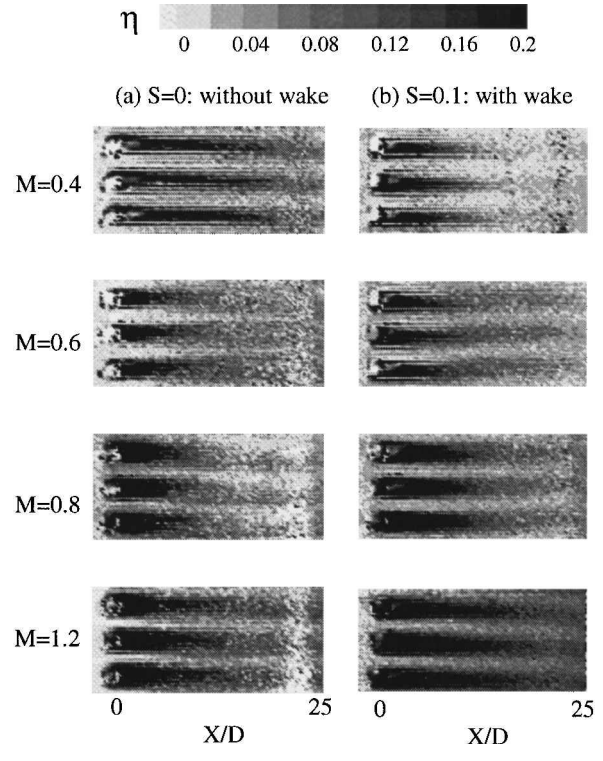

Fig. 3 Detailed film effectiveness distributions of fan-shaped holes for cases at different blowing ratios, with and without wake effect.

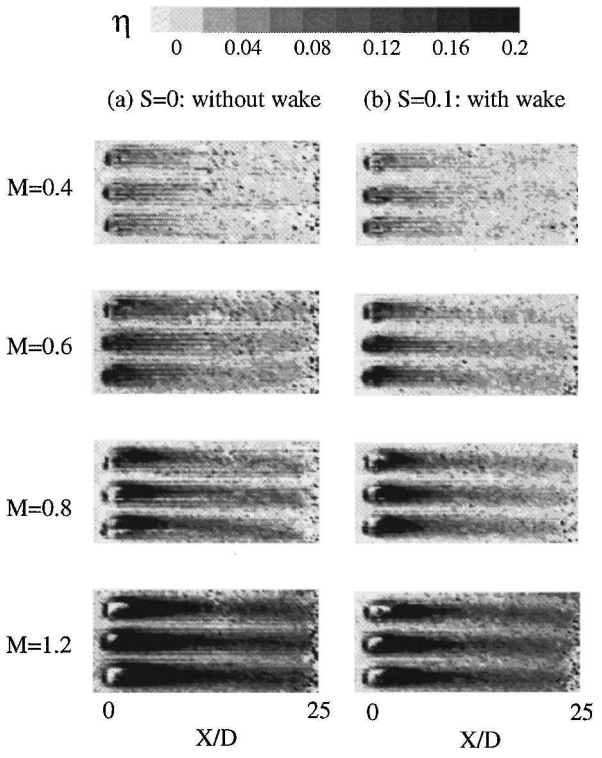

Fig. 4 Detailed film effectiveness distributions of laidback fan-shaped holes for cases at different blowing ratios, with and without wake effect.

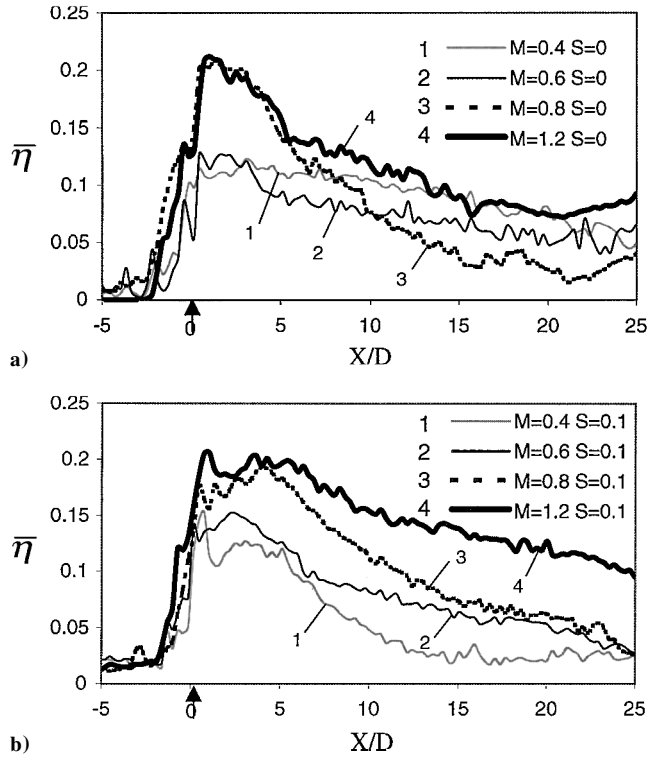

Fig. 5 Spanwise-averaged film effectiveness distribution of fan-shaped holes for a) steady flow, $S = 0.0$ and b) unsteady flow with wake effect, $S = 0.1$.

fan-shaped holes, respectively. Measurement are made on the three film holes in the middle of the row of nine film holes on the suction side. Because there are no data in the region from the leading edge to the film-hole location (here $X/D = 0$ is at film hole centerline) and the film effectiveness is very low after $X/D = 25$, the data capture area only covers the region from the upstream edge of the film holes to $X/D = 25$. The level for η is from 0 to 0.2. Note that in the jet center η has values up to 0.45.

Effect of Blowing Ratio

Because there are no film-cooling holes at the leading edge of the blade model, the film streaks start where the row of film-cooling holes (the only row of holes in this study) is located. Wider film steaks extend along the streamwise direction fairly straightly. The streaks are gradually weakened as they extend further away from the film-cooling holes. For the cases without unsteady wake effects ($S = 0$), the film effectiveness of the fan-shaped holes (Fig. 3a) decreases at first with the increase of blowing ratio. The film streaks are observable from $X/D = 0$ to 20 for a blowing ratio of $M = 0.4$. The observable streaks reduce considerably as the blowing ratio increases to $M = 0.6$. For the case of $M = 0.8$, the film streaks become even shorter but wider. The film coverage area increases again as the blowing ratio increases further to $M = 1.2$. The case of $M = 1.2$ provides the best thermal protection over the blade surface compared to all of the other three lower blowing ratios. For the laidback fan-shaped holes (Fig. 4a) the film coverage area increases with the increase of blowing ratio over the blade surface. Compared with fan-shaped holes, the blowing ratio has a monotonic effect on the film protection area for laidback fan-shaped holes: the film coolant trace is barely seen for low blowing ratio of $M = 0.4$, whereas the highest blowing ratio case of $M = 1.2$ produces downstream of the film-cooling holes a coolant trace, which is even stronger than that produced by fan-shaped holes.

Effect of Unsteady Wake

For fan-shaped holes with unsteady wake effects (Fig. 3b), the coolant jet dilutes faster into the mainstream, and the film protection in the front area decreases for cases with lower blowing ratios ($M = 0.4$ and 0.6) than the cases without wake effects. Only a small front portion ($X/D < 10$) of the suction surface is covered by the film-cooling jet. However, with unsteady wake effect, film coverage in the front area increases for cases of higher blowing ratios ($M = 0.8$ and 1.2). For laidback fan-shaped holes (Fig. 4b) unsteady wake has reduced film effectiveness for all blowing ratios.

All this indicates that unsteady wake has a strong effect on the film-cooling protection area. Generally, addition of unsteady wake results in lower film-cooling effectiveness at the area downstream of film hole as a result of the intensive mixing between mainstream and coolant jet, except for the case of high blowing ratio near fan-shaped holes.

Spanwise-Averaged Film Effectiveness Distributions

Figures 5 and 6 present the spanwise-averaged film effectiveness distribution for fan-shaped and laidback fan-shaped holes.

Effect of Blowing Ratio

For cases without unsteady wake effect (Figs. 5a and 6a), it is observed that, for all blowing ratio cases, spanwise-averaged film effectiveness decreases from $X/D = 0$ to 25. For fan-shaped holes (Fig. 5a) the spanwise-averaged film effectiveness decreases with the increase of blowing ratio but increases again when blowing ratio increases to 1.2. For laidback fan-shaped holes (Fig. 6a) spanwise-averaged film effectiveness increases with the increase of blowing ratio over the whole surface. Blowing ratio $M = 1.2$ produces the highest spanwise-averaged film effectiveness for both the fan-shaped and laidback fan-shaped holes.

Effect of Unsteady Wake

For fan-shaped holes (Fig. 5b) the addition of unsteady wake effect has made the spanwise-averaged film effectiveness decrease for lower blowing ratios of $M = 0.4$ and 0.6. For higher blowing ratios of $M = 0.8$ and 1.2, the spanwise-averaged film effectiveness increases from $X/D = 0$ to 25. For laidback fan-shaped holes (Fig. 6b) the unsteady wake effect makes the spanwise-averaged film effectiveness decrease for all blowing ratios.

From both Figs. 5 and 6 we conclude that, in general, the spanwise-averaged film effecitiveness increases with increasing

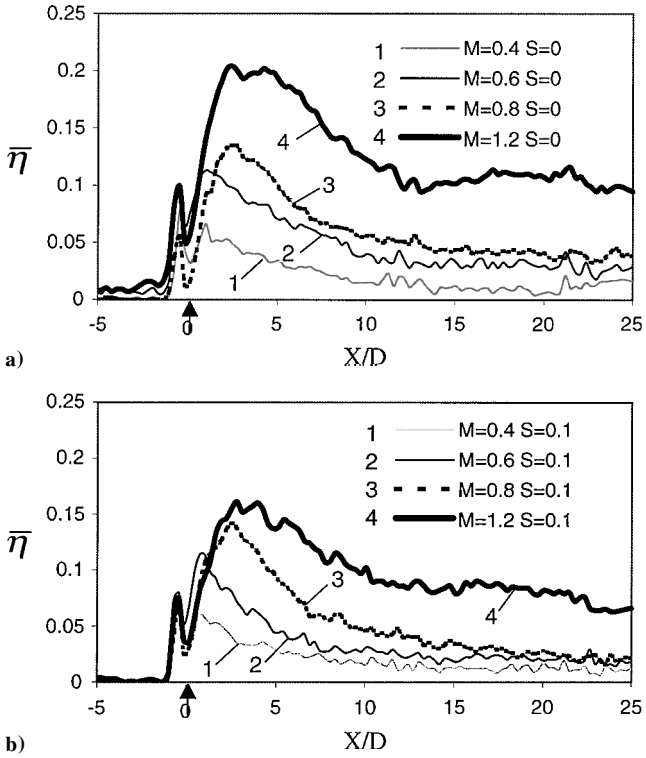

Fig. 6 Spanwise-averaged film effectiveness distributions of laidback fan-shaped holes for a) steady flow, $S = 0.0$ and b) unsteady flow with wake effect, $S = 0.1$.

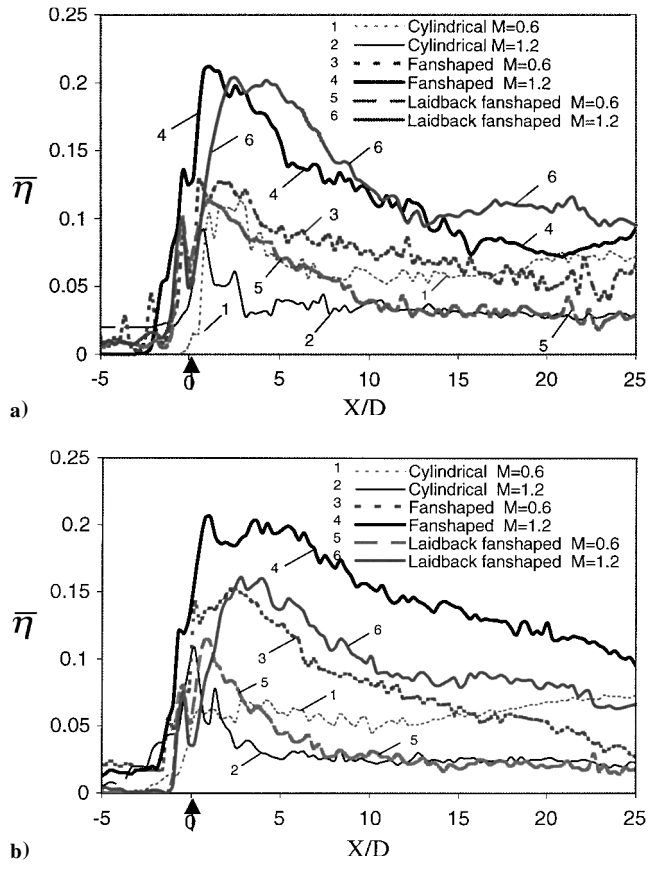

Fig. 7 Effect of hole shape on spanwise-averaged film effectiveness distributions for a) steady flow without wake effect, $S = 0.0$ and b) unsteady flow with wake effect, $S = 0.1$.

blowing ratio for both types of shaped holes, except for the steady flow case of $M = 0.4$ for fan-shaped holes. This case is repeatable. We cannot offer a satisfying explanation for this special case for the time being, though we suspect that it might caused by a higher uncertainty for low blowing ratio cases.

Effect of Hole Shape

Figure 7 compares the spanwise-averaged film effectiveness distributions of fan-shaped and laidback fan-shaped holes with that of standard cylindrical holes[15] for X/D up to 25 downstream of film hole. For cases without unsteady wake effect (Fig. 7a) with a high blowing ratio of $M = 1.2$, the spanwise-averaged film effectiveness of laidback fan-shaped holes is slightly higher than that of fan-shaped holes but much higher than that of cylindrical holes. For cases without unsteady wake effect with a low blowing ratio of $M = 0.6$, the spanwise-averaged film effectiveness of fan-shaped holes is slightly higher than that of laidback fan-shaped holes but much higher than that of cylindrical holes. For cases with unsteady wake effect (Fig. 7b), the spanwise-averaged film effectiveness of fan-shaped holes is higher than that of laidback fan-shaped holes and subsequently much higher than that of cylindrical holes for both low and high blowing ratios. This concludes that both fan-shaped and laidback fan-shaped holes have much better thermal protection than cylindrical holes under both steady and unsteady flow conditions. Particularly, fan-shaped holes provide the best thermal protection for all cases except for the steady flow case of $M = 1.2$, in which the laidback fan-shaped holes provide better thermal protection (higher film effectiveness). The explanation is that, at large blowing ratios, coolant coming out of a film hole has large momentum and tends to lift off into the mainstream. The exit forward expansion angle of a laidback fan-shaped hole has a larger cross section and reduces the coolant exit momentum, thus providing better thermal protection for this case. The conclusion of this section confirms the observation from Gritsch et al.[21] Generally the film-cooling effectiveness of this study is lower than that presented by Gritsch et al.[21] This may be caused by a larger inclined angle of film hole, 40 deg used by this study vs 30 deg used by Gritsch et al.,[21] as well as the convex surface of a turbine blade in this study compared to a flat surface in the other study.

Spanwise-Averaged Heat-Flux Ratio Distributions

Figure 8 presents the effect of hole shape on spanwise-averaged heat-flux ratio for $M = 0.6$. The information on h and h_0 is obtained from Teng et al.[24] The small arrow at $X/D = 0$ indicates the film injection location. The first three lines (1, 2, 3) in Fig. 8 compare the film-hole shape effects under steady flow condition. For film injection through fan-shaped holes, the spanwise-averaged heat-flux ratio ($\bar{q}''/\bar{q}''_0$) drops to as low as 0.5 at $X/D = 2$. The spanwise-averaged heat-flux ratio remains less than 0.8 from $X/D = 0$ to 10. Fan-shaped hole film injection greatly reduces heat transfer in this region. For film injection through laidback fan-shaped holes, the spanwise-averaged heat-flux ratio has a value varying between 0.8 and 0.9 from $X/D = 0$ to 15. However, for film injection through cylindrical holes, the spanwise-averaged heat flux ratio is about 0.9 from $X/D = 0$ to 7. In fact, the spanwise-averaged heat-flux ratio for cylindrical hole injection is larger than 1 in the range from $X/D = 8$ to 13, which indicates that the heat transfer is enhanced in that region. In the range from $X/D = 0$ to 15, the spanwise-averaged heat flux of fan-shaped hole film injection has a lower value than laidback fan-shaped hole film injection and thus a much less value than cylindrical hole film injection. For a low blowing ratio of $M = 0.6$, the coolant coming out of laidback fan-shaped holes mixes with and dilutes faster into the mainstream, leading to higher surface heat-flux ratio (and thus worse surface protection) than fan-shaped holes. The spanwise-averaged heat-flux ratio for all of the three kinds of injection is about 1 after $X/D = 15$. The last three lines (4, 5, 6) in Fig. 8 compare the hole-shape effects under unsteady flow condition. The general trend is the same as the cases under steady flow condition. However, the spanwise-averaged heat-flux ratio is reduced for all of the three types of film hole injection.

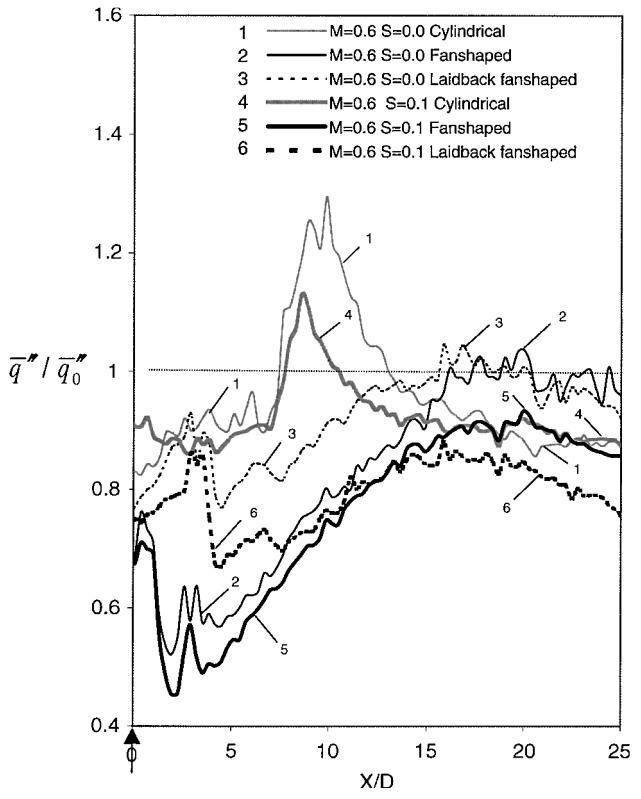

Fig. 8 Effect of hole shape on spanwise-averaged heat-flux ratio for $M = 0.6$ at steady flow ($S = 0.0$) and unsteady flow with wake effect ($S = 0.1$).

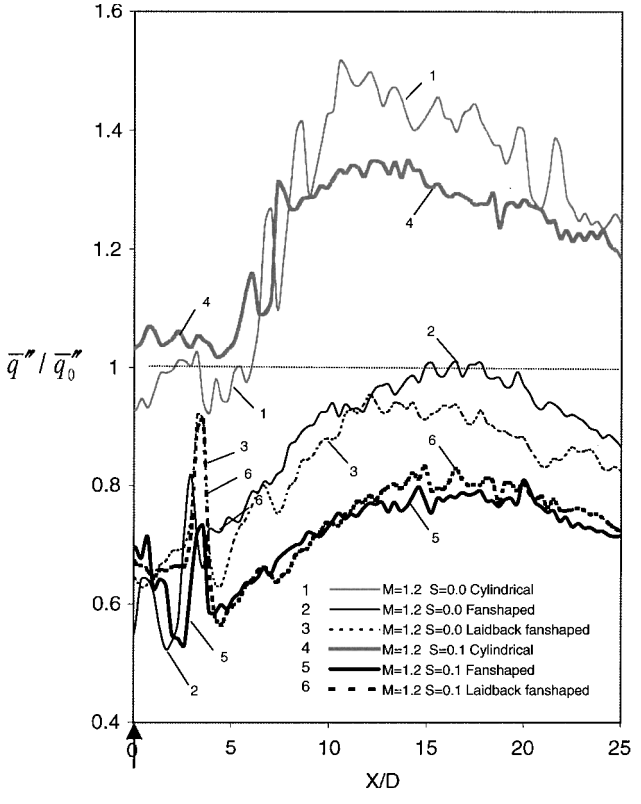

Fig. 9 Effect of hole shape on spanwise-averaged heat-flux ratio for $M = 1.2$ at steady flow ($S = 0.0$) and unsteady flow with wake effect ($S = 0.1$).

This indicates that the heat transfer between the mainstream and the blade surface is reduced by film injection for all of the cases when there is unsteady wake effect. Film injection through fan-shaped and laidback fan-shaped holes provides an even better film protection than cylindrical hole injection under unsteady flow condition. This proves that film jets coming out of holes with expanded exits, that is, with reduced jet momentum, can stay closer to the blade surface and avoid strong mixing with the mainstream and thus provide better film-cooling performance.

Figure 9 presents the effect of hole shape on spanwise-averaged heat-flux ratio for $M = 1.2$. Film injection through cylindrical holes does not provide any thermal protection over the blade surface at all. Actually, because of an increased spanwise-averaged heat-flux ratio all of the way from $X/D = 0$ to 25, cylindrical hole injection enhances surface heat transfer and worsens the surface condition. On the other hand, with an increased blowing ratio of $M = 1.2$, the film-cooling performance of both fan-shaped and laidback fan-shaped hole injections becomes even better. Both types of fan-shaped hole injection have almost the same values for both unsteady and steady flow conditions, respectively. Under steady flow condition the spanwise-averaged heat-flux ratio is 0.6 at film injection location. The value gradually increases to 0.9 at $X/D = 15$ and slightly decreases afterwards. Under unsteady flow condition the spanwise-averaged heat-flux ratio is around 0.7 all the way from $X/D = 0$ to 25, except a small fluctuation around $X/D = 3$. For a high blowing ratio of $M = 1.2$, film injection through fan-shaped

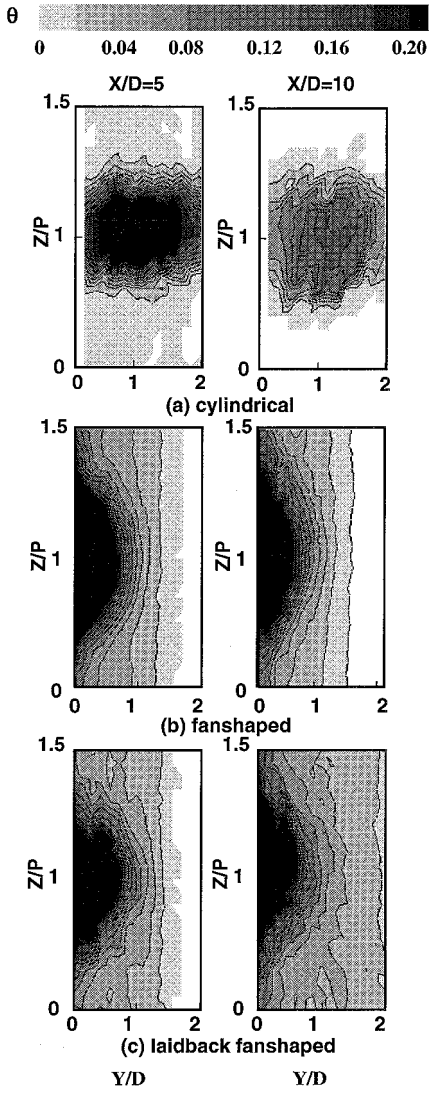

Fig. 10 Effect of hole shape on detailed film temperature profiles for steady flow ($S = 0.0$) at $M = 1.2$.

and laidback fan-shaped holes provides an even better film protection than cylindrical hole injection under unsteady flow condition.

In general, both fan-shaped and laidback fan-shaped film-hole injection provides lower spanwise-averaged heat-flux ratio and thus better thermal protection over the blade surface, especially under unsteady flow condition. With an increased blowing ratio film injection through both types of fan-shaped holes provides much lower spanwise-averaged heat-flux ratio and thus better cooling performance than cylindrical holes. Overall, fan-shaped holes provide better thermal protection than laidback fan-shaped holes for all cases, except for the steady flow case of $M = 1.2$, in which the laidback fan-shaped holes provide better thermal protection (lower heat-flux ratio). This may be because that, at large blowing ratios, coolant coming out of a film hole has large momentum and tends to lift off into the mainstream. The exit forward expansion angle of a laidback fan-shaped hole has a larger cross section and reduces the coolant exit momentum, thus providing better thermal protection in this case.

Coolant Jet Temperature Field Measurements

Figures 10 and 11 present the effect of hole shape on film temperature field for steady flow and unsteady flow with wake effect, respectively. The selected blowing ratio is $M = 1.2$. The film temperature field is measured at two locations: $X/D = 5$ and 10. The level for θ is from 0 to 0.2 with regard to η. In the jet center θ has values up to 0.45. The figures show that the nondimensional temperature distributions measured in the flow match the surface film-cooling effectiveness distributions as the wall is approached.

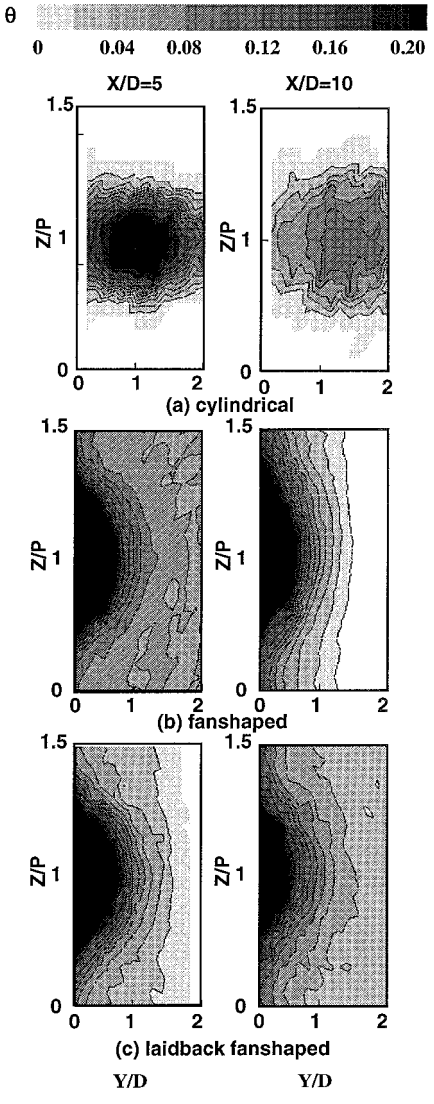

Fig. 11 Effect of hole shape on detailed film temperature profiles for unsteady flow with wake effect ($S = 0.1$) at $M = 1.2$.

Effect of Hole Shape

Temperature contours (Fig. 10) dilute as the heated coolant jet moves away from the eject location as a result of the mixing between heated jet and cold freestream air. Film jet coming out of cylindrical holes tends to lift off into the mainstream flow, with the jet periphery barely touching the blade surface. The film coverage area is very narrow in spanwise direction (small Z/P) but long in boundary-layer direction (large Y/D). On the other hand, both fan-shaped and laidback fan-shaped holes present much better and wider coolant protection over blade spanwise surface (Z/P), with the coolant jet attached closely to the surface and also spreading out along the spanwise direction, that is, there is increased coverage in Z/P direction but reduced jet penetration into mainstream in Y/D direction. Actually, the film jets coming out of the adjacent fan-shaped holes expand so widely in the spanwise direction so that their peripheries almost merge into each other, thus providing an almost continuous protection (greater Z/P) over the whole blade surface. Once again, the film-cooling behavior of laidback fan-shaped holes is not found to be better than that of fan-shaped holes in the film temperature field measurement. Because of too much expansion in both spanwise and streamwise directions, the laidback fan-shaped holes have reduced coolant protection in spanwise direction, that is, reduced Z/P coverage, but increased jet penetration into mainstream in Y/D direction as compared with the fan-shaped holes.

Effect of Unsteady Wake

Film jets for cases with unsteady wake effect dilute faster (Fig. 11), which has also been illustrated by the detailed film effectiveness distributions. Unsteady wake has a greater effect on the film temperature field of cylindrical holes than those of fan-shaped and laidback fan-shaped holes. This is because the film jet coming out of cylindrical holes lift off into the mainstream flow, resulting in larger contacting area as well as more intensive mixing between mainstream and coolant jet. Film jets coming out of fan-shaped and laidback fan-shaped holes tend to attach closely to the blade surface. They are mainly within the boundary layer of the mainstream, and the mixing between the mainstream and the coolant is not very strong.

Conclusions

Detailed coolant jet temperature profiles and film effectiveness distributions on the suction side of a gas turbine blade are measured using a thermocouple probe and a transient liquid crystal image method, respectively. The blade has only one row of film holes near the gill-hole portion on the suction side of the blade. The hole geometries studied include standard cylindrical holes and holes with diffuser-shaped exit portion (i.e., fan-shaped holes and laidback fan-shaped holes). The mainstream Reynolds number based on cascade exit velocity is 5.3×10^5. Upstream unsteady wakes are simulated using a spoke-wheel-type wake generator. Wake Strouhal number is kept at 0 or 0.1. Coolant blowing ratio is varied from 0.4 to 1.2. The conclusions based on the experimental results are the following:

1) For the blowing ratio range used in this study, fan-shaped and laidback fan-shaped holes provide better film-cooling effectiveness for both steady flow and unsteady flow with wake effects. The spanwise-averaged film effectiveness of fan-shaped and laidback fan-shaped holes can be up to two times of that of cylindrical holes.

2) In general, fan-shaped holes provide better film-cooling effectiveness than laidback fan-shaped holes and subsequently much better than cylindrical holes.

3) For cylindrical holes film-cooling effectiveness decreases as the blowing ratio increases from 0.6 to 1.2. However, for fan-shaped and laidback fan-shaped holes, film-cooling effectiveness increases as the blowing ratio increases from 0.6 to 1.2.

4) Unsteady wake tends to decrease film-cooling effectiveness, except for the higher blowing ratio cases ($M = 0.8$ and 1.2) from

$X/D = 0$ to 25 of fan-shaped holes, where the film-cooling effectiveness increases.

5) In general, both fan-shaped and laidback fan-shaped film-hole injection provides lower spanwise-averaged heat-flux ratio and thus better thermal protection over the blade surface, especially under unsteady flow condition. With an increased blowing ratio film injection through both kinds of fan-shaped holes provides much lower spanwise-averaged heat-flux ratio and thus better cooling performance than cylindrical holes.

6) The film effectiveness distribution measured with the liquid crystal technique provides the detailed information about the variation of film effectiveness along both the streamwise and the spanwise direction, whereas the coolant jet temperature profiles measured with the thermocouple probe help to explain and confirm the fact that fan-shaped and laidback fan-shaped holes have better film-cooling performance than cylindrical holes.

Acknowledgments

This paper is prepared with the support of the NASA Lewis Research Center under Grant Number NAG3-1656. The NASA technical team is Philip E. Poinsatte and Raymond Gaugler. Their support is greatly appreciated.

References

[1]Nirmalan, V., and Hylton, L., "An Experimental Study of Turbine Vane Heat Transfer with Leading Edge and Downstream Film Cooling," *Journal of Turbomachinery*, Vol. 112, No. 3, 1990, pp. 477–487.

[2]Abuaf, N., Bunker, R., and Lee, C. P., "Heat Transfer and Film Cooling Effectiveness in a Linear Airfoil Cascade," American Society of Mechanical Engineers, Paper 95-GT-3, June 1995.

[3]Ames, F. E., "Aspects of Vane Film Cooling with High Turbulence: Part I—Heat Transfer," American Society of Mechanical Engineers, Paper 97-GT-239, June 1997.

[4]Ames, F. E., "Aspects of Vane Film Cooling with High Turbulence: Part II—Adiabatic Effectiveness," American Society of Mechanical Engineers, Paper 97-GT-240, June 1997.

[5]Drost, U., and Bölcs, A., "Investigation of Detailed Film Cooling Effectiveness and Heat Transfer Distributions on a Gas Turbine Airfoil," American Society of Mechanical Engineers, Paper 98-GT-20, June 1998.

[6]Camci, C., and Arts, T., "An Experimental Convective Heat Transfer Investigation Around a Film-Cooled Gas Turbine Blade," *Journal of Turbomachinery*, Vol. 112, No. 3, 1990, pp. 497–503.

[7]Takeishi, K., Aoki, A., Sato, T., and Tsukagoshi, K., "Film Cooling on a Gas Turbine Rotor Blade," *Journal of Turbomachinery*, Vol. 114, No. 4, 1992, pp. 828–834.

[8]Ito, S., Goldstein, R. J., and Eckert, E. R. G., "Film Cooling of a Gas Turbine Blade," *Journal of Engineering for Power*, Vol. 100, No. 3, 1978, pp. 476–481.

[9]Haas, W., Rodi, W., and Schönung, B., "The Influence of Density Difference Between Hot and Coolant Gas on Film Cooling by a Row of Holes: Predictions and Experiments," *Journal of Turbomachinery*, Vol. 114, No. 4, 1992, pp. 747–755.

[10]Abhari, R. S., and Epstein, A. H., "An Experimental Study of Film Cooling in a Rotating Transonic Turbine," *Journal of Turbomachinery*, Vol. 116, No. 1, 1994, pp. 63–70.

[11]Ou, S., Han, J. C., Mehendale, A. G., and Lee, C. P., "Unsteady Wake over a Linear Turbine Blade Cascade with Air and CO_2 Film Injection: Part I—Effect on Heat Transfer Coefficients," *Journal of Turbomachinery*, Vol. 116, No. 4, 1994, pp. 721–729.

[12]Mehandale, A. B., Han, J. C., Ou, S., and Lee, C. P., "Unsteady Wake over a Linear Turbine Blade Cascade with Air and CO_2 Film Injection: Part II—Effect on Film Effectiveness and Heat Transfer Distributions," *Journal of Turbomachinery*, Vol. 116, No. 4, 1994, pp. 730–737.

[13]Du, H., Han, J. C., and Ekkard, S. V., "Effect of Unsteady Wake on Detailed Heat Transfer Coefficient and Film Effectiveness Distributions for a Gas Turbine Blade," *Journal of Turbomachinery*, Vol. 120, No. 4, 1998, pp. 808–817.

[14]Du, H., Ekkad, S. V., and Han, J. C., "Effect of Unsteady Wake with Trailing Edge Coolant Ejection on Film Cooling Performance for a Gas Turbine Blade," *Journal of Turbomachinery*, Vol. 121, No. 3, 1999, pp. 448–455.

[15]Teng, S., Sohn, D. K., and Han, J. C., "Unsteady Wake Effect on Film Temperature and Effectiveness Distributions for a Gas Turbine Blade," *Journal of Turbomachinery*, Vol. 122, No. 2, 2000, pp. 340–347.

[16]Goldstein, R., Eckert, E., and Burggraf, F., "Effects of Hole Geometry and Density on Three-Dimensional Film Cooling," *International Journal of Heat and Mass Transfer*, Vol. 17, No. 4, 1974, pp. 595–607.

[17]Makki, Y., and Jekubowski, G., "An Experimental Study of Film Cooling from Diffused Trapezoidal Shaped Holes," AIAA Paper 86-1326, June 1986.

[18]Haller, B., and Camus, J., "Aerodynamic Loss Penalty Produced by Film Cooling Transonic Turbine Blades," American Society of Mechanical Engineers, Paper 83-GT-77, March 1983.

[19]Schmidt, D., Sen, B., and Bogard, D., "Film Cooling with Compound Angle Holes: Adiabatic Effectiveness," American Society of Mechanical Engineers, Paper 94-GT-312, June 1994.

[20]Sen, B., Schmidt, D. L., and Bogard, D. G., "Film Cooling with Compound Angle Holes: Heat Transfer," American Society of Mechanical Engineers, Paper 94-GT-311, June 1994.

[21]Gritsch, M., Schulz, A., and Wittig, S., "Adiabatic Wall Effectiveness Measurements of Film-Cooling Holes with Expanded Exits," American Society of Mechanical Engineers, Paper 97-GT-164, June 1997.

[22]Gritsch, M., Schulz, A., and Wittig, S., "Heat Transfer Coefficient Measurements of Film-Cooling Holes with Expanded Exits," American Society of Mechanical Engineers, Paper 98-GT-28, June 1998.

[23]Bell, C. M., Hamakawa, H., and Ligrani, P. M., "Film Cooling from Shaped Holes," *Journal of Heat Transfer*, Vol. 122, No. 2, 2000, pp. 224–232.

[24]Teng, S., Han, J. C., and Poinsatte, P. E., "Effect of Film-Hole Shape on Turbine Blade Heat Transfer Coefficient Distribution," *Journal of Thermophysics and Heat Transfer*, Vol. 15, No. 3, 2001, pp. 249–256.

[25]Mehandale, A. B., and Han, J. C., "Influence of High Mainstream Turbulence on Leading Edge Film Cooling Heat Transfer," *Journal of Turbomachinery*, Vol. 110, No. 1, 1992, pp. 66–72.